Counterion Condensation on a Helical Charge Lattice

Gerald S. Manning

Department of Chemistry, Rutgers University, 610 Taylor Road, Piscataway, New Jersey 08854-8087

Received January 30, 2001; Revised Manuscript Received April 20, 2001

ABSTRACT: We extend the theory of counterion condensation from the standard representation of a locally stiff rodlike polyion as a line of discrete charges to a helical lattice of charges. The number of counterions condensing on a helix with given axial charge density is the same as on a line of the same charge density, but the electrostatic free energy is substantially less for the helix than for the line. In fact, the free energy of assembling the helical charge lattice becomes negative at higher salt concentrations, indicating electrostatic stabilization of the helix due to the mixing entropy of condensed counterions. The electrostatic persistence lengths of the line and helix subjected to locally elastic thermal bending fluctuations differ only slightly. They have the same κ^{-2} dependence as the Odijk−Skolnick−Fixman persistence length but a different prefactor. It is commonly believed that elastic bending models for the persistence length are applicable to double-helical DNA, but we point out that DNA apparently has unique mechanical properties that do not conform to the elastic model of bending. On the other hand, the helical model and its subsequent generalization to a double helix will serve as a basis for the electrostatic free energy of DNA conformational transitions.

1. Introduction

The layer of counterions predicted by theory to condense on locally rodlike polyions[1,2] has been directly visualized in Monte Carlo simulations of DNA and its counterions,[3] and the renormalization of polymer charge by condensed counterions—that is, the effective reduction of polymer charge by exactly the charge of the condensed layer—is the simplest and most obvious interpretation of the invariance of position, intensity, and shape of the polyelectrolyte scattering peak for a family of flexible charged polymers with varying charge density.[4] The condensed layer is predicted to emerge only above a threshold polyion charge density, and the invariance of the SANS scattering peak is indeed observed only above the predicted threshold.[4] For the standard *B* form of DNA, the predicted number of condensed monovalent counterions is 0.76 per DNA phosphate charge, independent of added salt concentration.[5] Molecular dynamics trajectories of *B* DNA, counterions, and water molecules feature a count of 0.76 Na^+ ions per phosphate within an inflection in the integrated counterion distribution in the absence of added salt,[3] while other MD simulations with 0.8 M added NaCl find 0.70 excess Na^+ ions in a primary close peak of the counterion radial distribution function.[6] A variety of other measurements and simulations directed at detection of counterion condensation have been reviewed.[1]

There is in a sense a discrepancy between the theory on one hand and the measurements and simulations on the other. While the latter are performed on structured and semiflexible polyions in the presence of real counterions and real water molecules, the theory has traditionally rested on an infinite line of discrete point charges, point counterions, and a solvent continuum. Why should such good agreement of prediction with measurement be encountered? A thorough analysis of the theoretical length dependence has revealed that the number of counterions condensed on a line of length the same order as the Debye screening length is the same as for lines much longer than the screening length.[7] Since Debye length segments of a flexible polyion are expected to be more or less fully extended, it is perhaps not so surprising that the charge renormalization predicted for "infinite" lines should be realized by flexible as well as stiff polyions. Further, the number of condensed counterions is determined by long-range electrostatics, so a structureless model is not inappropriate. But although this last statement is intuitively acceptable, a quantitative theoretical underpinning has not before been available.

The primary purpose of this paper is to generalize counterion condensation theory from the model of a line of discrete charges to a polyion model of discrete charges placed uniformly along a helical trajectory, the latter serving as an example of a locally stiff polyion with realistic structure. We will thus make transparent those results of counterion condensation theory that are model-independent and those that are not. As a first application, we look at the persistence lengths of the two types of charge arrays subjected to smooth thermal bending fluctuations. Other applications and extensions of the helical model are envisaged for subsequent report, especially in the field of DNA conformational transitions and protein binding.

In the next section, we review salient features of the line-charge model and add new material on its persistence length. Then we develop the parallel theory of the helical charge lattice, including its electrostatic free energy and its persistence length. The results are presented as analytical formulas and portrayed graphically using numerical values of structural parameters characteristic of one of the helices in double-helical *B*-form DNA. The conditions for validity of the predicted free energy are discussed in some detail, namely, that the length of the helix be greater than the Debye screening length and that the axial charge spacing be less than the Debye length.

2. The Line Charge

The model polyion, isolated in a bath of solvent and salt, is a straight linear array of unit charges of the same sign with spacing b.[5,8] The length of the polyion

10.1021/ma010159b CCC: $20.00
Published on Web 05/25/2001

is assumed greatly to exceed the Debye screening length $1/\kappa$.[7] The unsigned unit charge is q, but each charge is effectively reduced by θ condensed counterions of unsigned valence Z to the value $(1 - Z\theta)q$, θ to be determined as the number of condensed counterions per unit charge. In this and subsequent sections, the following infinite series is central. It is a sum of Debye–Hückel interactions between pairs of unit charges on the polyion,

$$SUM = \sum_{n=1}^{\infty} \frac{e^{-\kappa r_n}}{r_n} \tag{1}$$

where r_n is the distance between a pair of unit charges separated by $n - 1$ other charges along the polymer chain. A first component g_1 of the polyelectrolyte free energy per unit charge is SUM with prefactor corresponding to the *effective* charge,

$$g_1/k_BT = (1 - Z\theta)^2 l_B SUM \tag{2}$$

where l_B is the Bjerrum length q^2/Dk_BT and D the dielectric constant of solvent.

For the line of unit charges, r_n is equal to nb, and SUM may be represented by a closed formula.[5] Isolation of a logarithmically divergent term leads to an expression for the first free energy component,

$$g_1/k_BT = -(1 - Z\theta)^2 \xi \ln(\kappa b) - (1 - Z\theta)^2 \xi \ln \frac{1 - e^{-\kappa b}}{\kappa b} \tag{3}$$

where $\xi = l_B/b$ is the reduced linear polyion charge density based on the full charges q. Notice that the second term of eq 3 does not diverge (in fact, it vanishes) in the limit $\kappa b \rightarrow 0$.

The formula for κ^2 is $(8\pi) \times 10^{-3} N_{Av} l_B I$, where N_{Av} is Avogadro's number and I is the ionic strength of the salt in molarity. The ionic strength is proportional to salt molarity c and equals it if the salt is mono: monovalent. Therefore, the first term in eq 3 diverges like $-\ln c$ for dilute salt.

The second component of free energy g_2 is associated with the transfer of counterions from solution to the condensed layer on the polyion,

$$g_2/k_BT = \theta \ln \frac{1000\theta}{\gamma \nu c Q} \tag{4}$$

where Q is an internal partition function for the condensed layer (its units are cm^3 per mole of fixed charge). We include a bulk salt activity coefficient γ, and ν is the number of counterions in the chemical formula for the salt. The $-\ln c$ term in this expression represents the entropy of dissociation of a condensed counterion into bulk solution. It competes with the $-\ln c$ divergence of the electrostatic energy g_1.

The overall polyelectrolyte free energy per unit charge g equals $g_1 + g_2$, and to minimize it, its θ derivative is set to vanish with the approximation[8] that Q is independent of θ. In the resulting equation the two divergent $\ln c$ terms are combined. The combined $\ln c$ term and the remaining nondivergent terms are recognized as functionally independent and separately set to zero. With the $\ln c$ term equal to zero, it is immediately seen that θ vanishes below a threshold charge density $\xi^* = Z^{-1}$. Below this threshold there are no condensed counterions. Above the threshold, the minimizing value of θ is found not to vanish,

$$Z\theta = 1 - \frac{1}{Z\xi} \tag{5}$$

The reason for the occurrence of counterion condensation is that above the charge density threshold the process of transferring a counterion from bulk solution to the polyion involves a reduction of electrostatic energy greater than the loss of dissociation entropy, an atypical situation in the physical chemistry of ionic interactions brought about in the linear polyion system by the unusual entropy-like $-\ln c$ divergence of the dissociation energy.

When the nondivergent terms in the equilibrium equation $\partial g/\partial\theta = 0$ are set independently to zero, a self-consistent condition for the condensed layer partition function emerges.[5,8] With use of eq 5,

$$Q = 4\pi e N_{Av} b^3 Z' \frac{\nu + \nu'}{\gamma\nu}\left(\xi - \frac{1}{Z}\right)\left(\frac{1 - e^{-\kappa b}}{\kappa b}\right)^2 \tag{6}$$

where the primed quantities refer to the co-ion of the salt. See ref 8 for discussion of the physical meaning of this expression.

With the preceding formulas for θ and Q substituted into the free energy components, we have the minimized free energy of the line of discrete unit charges for charge densities above the condensation threshold $\xi > 1/Z$,

$$g/k_BT = -\frac{1}{Z}\left(2 - \frac{1}{Z\xi}\right)\ln(1 - e^{-\kappa b}) - \frac{1}{Z} + \frac{1}{Z^2\xi} \tag{7}$$

The apparent simplicity of this formula is perhaps deceptive. The coefficient of the screening term (the first term) is not linear in polyion charge density ξ, so it is more than Debye–Hückel linear screening. It is not invariant to ξ, so it is more than Debye–Hückel screening of charges renormalized to a constant value by condensed counterions. This term in fact incorporates the lost entropy of counterions brought from bulk into the condensed layer and also part of the internal free energy of the condensed counterions. Moreover, the additional terms $-Z^{-1} + (Z^2\xi)^{-1}$ have no counterpart in a linear theory, and the negative term $-Z^{-1}$ will loom large in the analysis and discussion to follow.

Accuracy of the free energy as calculated can be expected in only a limited range of salt concentrations. The Debye screening length κ^{-1} must be substantially larger than the charge spacing b; that is, κb must be less than unity.[5] This condition is almost obvious, since the free energy could not be a *polyelectrolyte* free energy, and the polyelectrolyte phenomenon of counterion condensation could not occur, if the screening length did not encompass many fixed charges. Mathematically, it would make no sense to treat expressions such as the one for g_1 in eq 3 as the sum of two independent terms if the first one were not large and the second one small. A separate analysis leads to the conclusion that small κb is also the condition that the local concentration of condensed counterions is larger than the counterion concentration in bulk solution.[5]

In Figure 1 we show a plot of g/k_BT as a function of the logarithm of κb. The value of the reduced charge density ξ is set at 2.11, corresponding to the axial phosphate spacing $b = 3.38$ Å of one of the strands of the *B* form DNA double helix. With b fixed at this value,

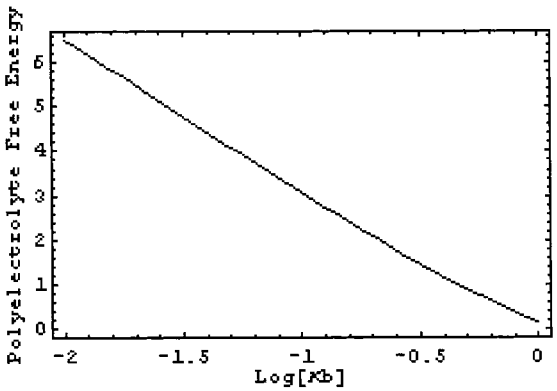

Figure 1. Electrostatic free energy of the line charge model in units of k_BT, eq 7 of text. The reduced charge density $\xi = 2.11$ at 25 °C in aqueous media and the spacing $b = 3.38$ Å conform to the structure of one of the helical strands in double-helical *B*-form DNA.

the plot gives the dependence on salt concentration. The mono:monovalent salt concentrations at the two extremes of the range shown are 8.1×10^{-5} and 0.81 M. The curve deviates perceptively from linearity only at the high concentration end, and as expected, it consists of positive values, indicating the requirement of work for assembly of the polyionic charge.

As an application, we calculate the polyelectrolyte contribution to the persistence length of the Landau–Lifshitz model, which assumes that any sufficiently short segment of a polymer chain bends like a linearly elastic rod into a circular arc.[9] To get a polyelectrolyte effect on bending fluctuations, this assumption must be coupled to a requirement that the "sufficiently short segment" be sufficiently long to be a polyelectrolyte; that is, its length must be longer than the Debye screening length. In our theory, as indicated above, we also need the screening length to be larger than the charge spacing. Finally, as will become clear in the calculation that follows, the screening length must be smaller than the radius of curvature of the bend.

Let our line of fixed charges be given a pure bend with uniform radius of curvature R, so that the charge spacing along the arc is invariant at the value b. The distance r_n between a pair of polyion charges separated by $n - 1$ other charges along the arc is now the length of the chord connecting the pair. Its formula is

$$r_n = \sqrt{2}R\left[1 - \cos\left(\frac{nb}{R}\right)\right]^{1/2} \tag{8}$$

Expanded about infinite R (straight line) out to the leading R^{-2} term, *SUM* in eq 1 may be evaluated analytically, and the Debye–Hückel free energy component eq 2 becomes

$$\frac{g_1(R)}{k_BT} = \frac{g_1^\infty}{k_BT} + (1 - Z\theta)^2\xi b^2 f(\kappa b)\frac{1}{R^2} \tag{9}$$

where the superscript ∞ refers to infinite radius of curvature, so that g_1^∞/k_BT is given by the right-hand side of eq 3, and

$$f(\kappa b) = \frac{1}{24}\frac{e^{-\kappa b}}{(1 - e^{-\kappa b})^3}[1 + \kappa b - e^{-\kappa b}(1 - \kappa b)] \tag{10}$$

Expanded for small κb, $f(\kappa b)$ equals $1/(8\kappa^2 b^2)$ to leading order. In the range up to $\kappa b = 1$, this simpler expression deviates from the closed formula eq 10 by at most 3%, and we therefore use it in the sequel instead of eq 10. In particular, we rewrite eq 9,

$$\frac{g_1(R)}{k_BT} = \frac{g_1^\infty}{k_BT} + \frac{(1 - Z\theta)^2\xi}{8\kappa^2R^2} \tag{11}$$

The second free energy component, the transfer of counterions to the condensed layer, is the same as in eq 4. The equilibrium condition with respect to counterion condensation on the bent polyion segment is $\partial[g_1(R) + g_2]/\partial\theta = 0$, and the left side of this equation again splits into a divergent $-\ln c$ term and terms that do not diverge. Among the terms that do not diverge—if in the divergent limit κ tends to zero and R to infinity such that the product κR is bounded away from zero—is the one that derives from the perturbation caused by slight bending (the second term on the right side of eq 11). In other words, the $-\ln c$ divergence is the same as for the straight line of charges, and the number of condensed counterions that minimizes the free energy of the bent segment is therefore the same as for the straight line, eq 5. The physical realization of the lower bound on κR is a slight bend with radius of curvature much greater than the screening length.

Although the number of condensed counterions for a slightly bent line turns out to be the same as for a straight line, the internal partition function Q of the condensed layer, that is, its local free energy, is changed by the bending. Independent vanishing of the nondivergent terms in the equilibrium condition leads to modification of Q in eq 6 for the straight line by the factor $1 - (4\kappa^2R^2)^{-1}$, where the second term is a perturbation on unity.

The minimized polyelectrolyte free energy for the slightly bent segment relative to its free energy when straight, that is, the reversible electrostatic work required for bending, can be written as follows (L is the length of the segment):

$$\Delta g(R) = \frac{1}{2}\frac{L}{R^2}\left[\frac{k_BT}{2Z\kappa^2 b}\left(1 - \frac{1}{2Z\xi}\right)\right] \tag{12}$$

whereupon the polyelectrolyte (electrostatic) contribution to the persistence length p_{el} can be read off as the Hooke's law bending modulus (the factor in brackets) divided by k_BT,

$$p_{el} = \frac{1}{2Z\kappa^2 b}\left(1 - \frac{1}{2Z\xi}\right) \tag{13}$$

Equation 13 is valid above the condensation threshold $\xi = Z^{-1}$. When there are no condensed counterions, $\xi < Z^{-1}$, the result we get is identical to Odijk–Skolnick–Fixman (OSF), $p_{el} = \xi/(4\kappa^2 b)$.[10,11] An apparently reasonable way to extend OSF to polyion charge densities above the condensation threshold is to renormalize the post-threshold density ξ to the threshold value Z^{-1}, thus obtaining the expression $1/(4Z\kappa^2 b)$ for p_{el} when $\xi > Z^{-1}$. This formula differs from the result we have just derived, eq 13. The salt concentration dependence is the same, but the prefactors differ by the factor $(2Z\xi - 1)/Z\xi$, equal to 1.76 for charge density corresponding to the *B*-DNA double helix ($\xi = 4.23$). The reason for the difference is that eq 13 accounts for the perturbation in the internal free energy of the condensed layer caused by bending as well as for charge renormalization. For a

similar reason, our present calculation supersedes our earlier attempt to apply counterion condensation theory to the persistence length problem, since we were then forced by the numerical procedure employed to neglect changes of the condensation volume with bending.[12]

3. The Helical Array of Charges

Consider as a polyion model a set of discrete unit charges arrayed uniformly along a helix. The position vector along the helical path is $\mathbf{r} = (a\cos\phi, a\cos\phi, h\phi)$, where a is the radius of the helix, h its rise, and ϕ the variable rotation angle. The projections of the charges onto the helical axis have uniform spacing b. The series of Debye−Hückel interactions, SUM in eq 1, continues to be a central quantity. The chord between a pair of charges separated by $n-1$ other charges along the helix has length

$$r_n = nb\left\{1 + \frac{2a^2}{n^2b^2}\left[1 - \cos\left(\frac{nb}{h}\right)\right]\right\}^{1/2} \tag{14}$$

and the Debye−Hückel component g_1 of the polyelectrolyte free energy is given by eq 2 with this expression for r_n in SUM. We can isolate a logarithmic divergence by adding and subtracting a line-charge summation, i.e., SUM with $r_n = nb$. For the helix we then get

$$g_1/k_BT = -(1 - Z\theta)^2\xi \ln(\kappa b) - (1 - Z\theta)^2\xi \ln\frac{1 - e^{-\kappa b}}{\kappa b} + (1 - Z\theta)^2\xi b\sum_{n=1}^{\infty}\left(\frac{e^{-\kappa r_n}}{r_n} - \frac{e^{-\kappa nb}}{nb}\right) \tag{15}$$

Notice that the first two terms are identical to the right side of eq 3; that is, they would be the entire free energy g_1/k_BT if the helical charge array were replaced by a linear array of charges projected from the helix onto its central axis. The first of these two terms diverges logarithmically as $\kappa \to 0$, and indeed this term is identical to the line-charge divergent term. The information that the charge array is helical is contained in the third term, the infinite series in which a line-charge interaction has been subtracted off in the summand. We emphasize this point below. Here, it is important to notice that the series does not diverge as $\kappa \to 0$. It converges, since the general term is easily shown to be $O(n^{-3})$.

The second free energy component g_2, which represents the thermodynamic consequences of transferring counterions from bulk into the condensed layer, is given by eq 4. Minimizing the total free energy $g_1 + g_2$ as described in the previous section results in the disclosure that the optimal number of condensed counterions continues to be given by eq 5, since it is determined exclusively by a $-\ln c$ divergence that is identical to the line charge divergence. The helical structure of the charge array is reflected not in the number of condensed counterions but in their free energy. It is the partition function Q that is modified from the line-charge result,

$$Q_{\text{helix}} = Q_{\text{line}} \exp(-2STRUCTURE) \tag{16}$$

where Q_{line} is the partition function of the counterions condensed on the line charge model, that is, the expression on the right side of eq 6, and

$$STRUCTURE = \sum_{n=1}^{\infty}\frac{1}{n}\left\{\frac{\exp\left[-\kappa nb\sqrt{1 + \frac{2a^2}{n^2b^2}\left(1 - \cos\left(\frac{nb}{h}\right)\right)}\right]}{\sqrt{1 + \frac{2a^2}{n^2b^2}\left(1 - \cos\left(\frac{nb}{h}\right)\right)}} - \exp(-\kappa nb)\right\} \tag{17}$$

The infinite series $STRUCTURE$ converges when $\kappa \to 0$ and carries the information that the charge array is a helix through the helical radius a and rise h. Note that $STRUCTURE$ becomes zero when the helix collapses to its axis, $a = 0$.

Finally, we have a formula for the minimized polyelectrolyte free energy of the helical array that follows from substitution of the above results for θ and Q into the components g_1 and g_2:

$$g/k_BT = \frac{1}{Z}\left(2 - \frac{1}{Z\xi}\right)[STRUCTURE - \ln(1 - e^{-\kappa b})] - \frac{1}{Z} + \frac{1}{Z^2\xi} \tag{18}$$

The right side equals g/k_BT for the line model plus the term proportional to $STRUCTURE$.

Figure 2 compares the free energy of the helical charge array with the line charge, the two arrangements of polyion charges having the same linear charge density. The radius and rise of the helix are taken as those of one of the helices in double-helical *B*-form DNA. Dispersal of the polyion charge from a line outward radially as in the helical array results in a lower free energy. Indeed, the free energy of the helical array becomes negative at the higher salt end of the curve. Commentary is deferred to the Discussion section. In the linear regions (lower salt concentrations), the line and helical models yield identical slopes, so limiting laws dependent on salt concentration are unaffected by a shift of model from line to helix (just as the number of condensed counterions does not change).

We can calculate the persistence length of the helical charge array subjected to smooth thermal bending fluctuations. The first step is to bend a finite cylinder to a toroidal arc. A helix embedded on the cylindrical surface is mathematically required not to slip as the cylinder bends, resulting in a well-defined curve winding around the torus. This curve is taken as the smoothly bent helix, and its free energy is calculated and compared to the free energy of the straight helix on the cylinder. The difference of these free energies determines the persistence length, in the same way as eq 12 determines the persistence length of the line model subjected to smooth bending. The calculation is long and tedious, and we proceed directly to the final result without provision of further detail. Thus, for the electrostatic persistence length $p_{\text{el}}^{\text{helix}}$ of the helical charge array, we obtain

$$p_{\text{el}}^{\text{helix}} = \frac{4}{Z}\left(1 - \frac{1}{2Z\xi}\right)\sum_{n=1}^{\infty}\frac{e^{-\kappa r_n}}{r_n}\sigma_n \tag{19}$$

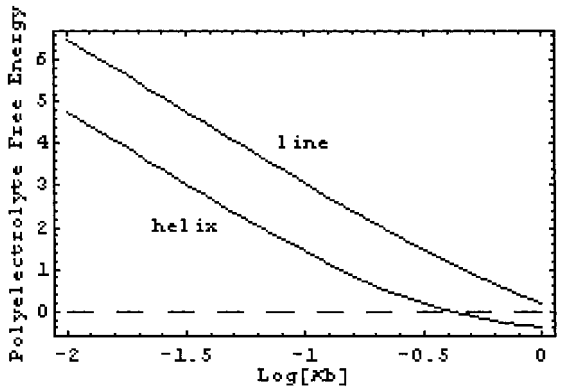

Figure 2. Electrostatic free energy of the helical charge lattice in units of k_BT, eq 18 of text, compared to the corresponding result for the line model taken from Figure 1. ξ and b as in caption to Figure 1. The helical radius $a = 9.23$ Å and rise $h = 5.37$ Å correspond to the structure of one of the helical stands in double-helical *B*-form DNA.

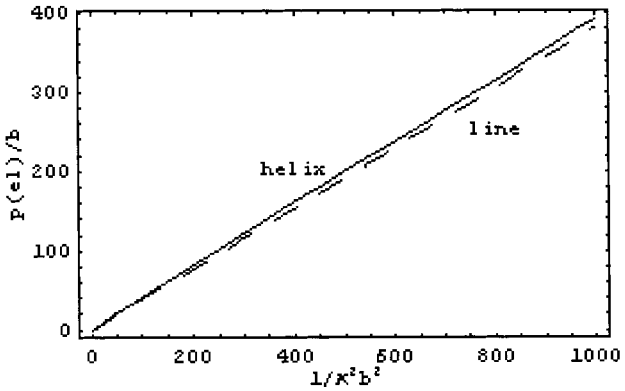

Figure 3. Persistence lengths of line and helical models, eq 13 and 19, respectively. Structural parameters as in captions to Figures 1 and 2.

where r_n is the length of the chord between two charges along the *straight* helix that are separated by $n - 1$ other charges, and is therefore given by eq 14, and where σ_n is the following expression:

$$\sigma_n = \frac{a^2}{4}\left(\frac{nb}{r_n}\right)^4\left[\frac{3}{2}(1+\kappa r_n) + \frac{1}{2}\kappa^2 r_n^{\,2} + \frac{r_n^{\,2}}{6a^2}(1+\kappa r_n) - \frac{1}{2}\cos\left(\frac{nb}{h}\right)(1+\kappa r_n+\kappa^2 r_n^{\,2}) - \frac{r_n^{\,2}}{n^2b^2}\cos\left(\frac{nb}{h}\right)(1+\kappa r_n)\right] \quad (20)$$

It can be checked that the persistence length of the helix collapses to that of the line, eq 13, when the helical radius a shrinks to zero.

Figure 3 shows a comparison of the persistence lengths of helix, eq 19, and line, eq 13, for DNA-like structural parameters. For the salt concentration range displayed, the difference is less than about 6%. Not only is the κ^{-2} dependence preserved by the helix, but the prefactors are also numerically close. Figure 2 demonstrated that the free energies of straight line and helix are substantially different. The free energies of bent line and bent helix (with the same radius of curvature) are also different, but by about the same amount as for the straight structures, so that the persistence lengths, which measure the energetic difference between bent and straight forms, are almost the same.

4. Discussion

Our primary goal has been to show how counterion condensation theory can be extended from its traditional model of a line of discrete charges to more realistic structures like a helical array of charges. Further generalizations to an intertwined double helix and applications of the double helix to problems in DNA physics, particularly structural transitions such as the "melting" of the double helix to single strands and the transitions between different double-helical conformations (*B* to *A*, *B* to *Z*, etc.), will be presented in subsequent reports.

An important result of the present paper is the demonstration that the number of condensed counterions depends only on the axial charge density of the helix and, indeed, is the same as for the standard line model of the same charge density. The derivation we give here makes the reason for this aspect of counterion condensation theory entirely transparent. The threshold condensation of counterions is a consequence of long-range electrostatics. At long range, only the part of the polyion field generated by the axial charge density of the helix is of consequence; the short-range part caused by the helical structure is not sensed. Thus, the logarithmic divergence that underlies condensation is identical for helix and line, and the analysis of the free energy component of eq 15 into a long-range part carrying the divergence and a convergent infinite series that would vanish but for the structural difference between a straight line and a helix with curvature and rise is the mathematical expression of this qualitative distinction between long- and short-range interactions.

Although the helical structure does not influence the number of condensed counterions (and hence does not change "limiting laws" dependent only on this number—note also the identical low-salt *slopes* in Figure 2), we also show as a second result that the internal free energy of the condensed layer does depend on the structure of the helix as indicated by eqs 16 and 17. This type of behavior was also seen in the Manning–Mohanty analysis of short oligoions.[7] The number of counterions condensed on a charged line of length the same order as the Debye screening length is the same as for a line much longer than the screening length (both being given by eq 5), but the internal free energy of the condensed layer is length-dependent.

Our third result is that the overall polyelectrolyte free energy of the helical array, that is, the work required to assemble the array from the isolated charges, is much smaller than for the line charge. It even becomes negative near the higher salt end of the range of validity of the theory (see Figure 2). It is important to realize that the range of salt concentrations in which the theories of the linear and helical charge arrays are expected to be accurate is the same, since the logarithmic divergences underlying counterion condensation in both models are identical. The divergence depends only on the *linear* charge density in both cases, and for both cases we expect reasonable accuracy up to salt concentrations such that κb approaches unity.[5] The graph of free energy for the helix in Figure 2 becomes negative at about $\kappa b = 0.3$. For double-helical DNA, ^{23}Na NMR detected no deviation from salt-independent counterion condensation up to the highest NaCl concentration examined, 0.6 M.[13] For the double helix, 0.6 M salt corresponds to $\kappa b = 0.4$. Molecular dynamics simulations[6] of the double helix with 0.8 M added salt, or κb

= 0.5, are quantitatively consistent with the predictions of counterion condensation (see Introduction).

A negative polyelectrolyte free energy is counterintuitive, since identical isolated charges are expected to repel each other as they are assembled from infinity onto the polyion. However, as just discussed, our result for the helical model should not be reflexively attributed to breakdown of the theory. In fact, the physical interpretation of the mathematical structure of our equations gives a picture that is not at all unreasonable. The feature of both eq 7 for the line model and eq 18 for the helical charge array that makes it possible for the free energy to become negative as salt concentration increases is the term $-Z^{-1}$, or -1 for monovalent counterions, common to both equations. For the line model, negative values are attained only at salt concentrations beyond the range of accuracy of the theory (4 M NaCl for an axial charge density characteristic of DNA). But for the helical model, the negative values of *STRUCTURE* in eq 18 allow overall negative free energy values to manifest themselves at lower salt concentrations. If we trace the origin of the -1 term in eq 18, we find that it stems from the term $\theta \ln \theta$ in the free energy component g_2 that accounts for the translational entropy of the condensed counterions. In the helical model, the electrostatic repulsions among the renormalized polyion charges are already sufficiently reduced by increasing salt at concentrations not high enough to destroy the integrity of the condensed layer of counterions. The favorable translational entropy of the condensed counterions then remains to endow the polyionic charge assembly with stability.

It is interesting that Patra and Yethiraj[14] have found free energy inversions in their density functional calculations on a "primitive" model polyion, but only for divalent or mixed salts, and for high axial charge densities that might be difficult to achieve experimentally.

As a new application of the line model, and as a first application of the helical model, we calculated the persistence lengths of both representations of an extended polyion subjected to thermal bending fluctuations. The line model yields the standard κ^{-2} dependence, i.e., inverse proportionality to salt concentration, of the Odijk−Skolnick−Fixman theory,[10,11] but above the condensation threshold the prefactor is different, because OSF does not account for the perturbation of the internal free energy of the condensed layer of counterions caused by bending. Our calculation for the helical charge array is presumably of some intrinsic interest, but the result of practical consequence seems to be that the helical structure scarcely affects the persistence length. The substantial effect of three-dimensional structure on the polyelectrolyte free energy seems to be about the same for straight and bent forms, so that Δg of bending, at least for the large radii of curvature pertinent to the persistence length, is only slightly perturbed.

Double-helical DNA is often invoked as the prototype of a semistiff polyion. We ourselves definitely plan to use the helical model as the basis for applications to the electrostatics of DNA conformational transitions. We wish to emphasize here, however, that the smooth linearly elastic bending underlying both the OSF theory and our present one of the electrostatic persistence length is probably not applicable to DNA, which may have unique mechanical properties. A number of years ago, we suggested that "null DNA", that is, a hypothetical DNA lacking ionic charge on its phosphate groups, would exist in a compact form, since segments of about 60 base pairs would not be mechanically stable with a straight axis but instead would be stably bent.[15,16] Null DNA appears now to have been observed in Kabanov's laboratory, and it is compact, unlike other polyelectrolytes observed in the same conditions.[17]

An underlying requirement for the persistence length theory presented in this paper is that local polyion segments conform to the physics of linearly elastic bending theory for thin straight rods. These segments must then be longer than the range of electrostatic interactions determined by the Debye screening length. For applicability of the smooth bending model, there must be internal stiffening forces other than those arising from the electrostatic crowding of ionic groups on the polymer. But for DNA it appears that the internal nonelectrostatic forces—far from acting to stiffen the double helix into an axially straight conformation—instead tend to fold it into a compact form.[17]

Acknowledgment. Our research is supported in part by PHS Grant GM36284.

References and Notes

(1) Manning, G. S. *Ber. Bunsen-Ges. Phys. Chem.* **1996**, *100*, 909−922.
(2) Ray, J.; Manning, G. S. *Macromolecules* **1999**, *32*, 4588−4595.
(3) Young, M. A.; Jayaram, B.; Beveridge, D. L. *J. Am. Chem. Soc.* **1997**, *119*, 59−69.
(4) Essafi, W.; Lafuma, F.; Williams, C. E. *Eur. Phys. J. B* **1999**, *9*, 261−266.
(5) Manning, G. S. *Q. Rev. Biophys.* **1978**, *11*, 179−246.
(6) Feig, M.; Pettitt, B. M. *Biophys. J.* **1999**, *77*, 1769−1781.
(7) Manning, G. S.; Mohanty, U. *Physica A* **1997**, *247*, 196−204.
(8) Manning, G. S. *Physica A* **1996**, *231*, 236−253.
(9) Landau, L. D.; Lifshitz, E. M. *Statistical Physics*; Pergamon: London, 1958.
(10) Odijk, T. *J. Polym. Sci.* **1977**, *15*, 477−483.
(11) Skolnick, J.; Fixman, M. *Macromolecules* **1977**, *10*, 944−948.
(12) Fenley, M. O.; Manning, G. S.; Olson, W. K. *J. Phys. Chem.* **1992**, *96*, 3963−3969.
(13) Anderson, C. F.; Record, M. T.; Hart, P. A. *Biophys. Chem.* **1978**, *7*, 301−316.
(14) Patra, C. N.; Yethiraj, A. *Biophys. J.* **2000**, *78*, 699−706.
(15) Manning, G. S. *Biopolymers* **1983**, *22*, 689−729.
(16) Manning, G. S. *J. Biomol. Struct. Dyn.* **1989**, *7*, 41−61.
(17) Sergeyev, V. G.; Pyshkina, O. A.; Lezov, A. V.; Mel'nikov, A. B.; Ryumtsev, E. I.; Zezin, A. B.; Kabanov, V. A. *Langmuir* **1999**, *15*, 4434−4440.

MA010159B